

Numerical analysis of the effect of side holes of a double J stent on flow rate and pattern

Kyung-Wuk Kim^a, Young Ho Choi^{b,*}, Seung Bae Lee^c, Yasutaka Baba^d, Hyung-Ho Kim^a and Sang-Ho Suh^a

^a*Department of Mechanical Engineering, Soongsil University, 369 Sangdo-Ro, Dongjak-gu, Seoul, 156-743, Korea*

^b*Department of Radiology and* ^c*Department of Urology, Seoul National University Boramae Hospital, 425 Shindaebang-2-dong, Dongjak-gu, Seoul, 156-707, Korea*

^d*Department of Radiology, Ryokusenkai Yonemori Hospital, 1-7-1, Yojiro, Kagoshima-shi, Kagoshima, 890-0062, Japan*

Abstract. A double J stent has been used widely these days for patients with a ureteral stenosis or with renal stones and lithotripsy. The stent has multiple side holes in the shaft, which supply detours for urine flow. Even though medical companies produce various forms of double J stents that have different numbers and positions of side holes in the stent, the function of side holes in fluid dynamics has not been studied well. Here, the flow rate and pattern around the side holes of a double J stent were evaluated in curved models of a stented ureter based on the human anatomy and straight models for comparison. The total flow rate was higher in the stent with a greater number of side holes. The inflow and outflow to the stent through the side holes in the curved ureter was more active than in the straight ureter, which means the flow through side holes exists even in the ureter without ureteral stenosis or occlusion and even in the straight ureter. When the diameter of the ureter changed, the in-stent flow rate in the ureter did not change and the extraluminal flow rate was higher in the ureter with a greater diameter.

Keywords: Ureter, stent, flow, CFD, numerical analysis

1. Introduction

The ureter is a part of the upper urinary system and is located between the kidney and bladder. Urine flows through the ureter from the kidney to the bladder. Ureteral stenosis or occlusion by intrinsic or extrinsic lesions causes the disturbance of normal urinary drainage, and flow diversion such as percutaneous nephrostomy or insertion of a ureteral stent is required to relieve it. In the case of renal stones, temporary placement of a ureteral stent is needed after lithotripsy. A double J stent among ureteral stents is widely used these days and many medical companies produce the stent [1-3]. A double J stent is composed of a shaft and proximal and distal coils, and it has multiple side holes

* Address for correspondence: Young Ho Choi, Department of Radiology, Seoul National University Boramae Hospital, 425 Shindaebang-2-dong, Dongjak-gu, Seoul, 156-707, Korea. Tel.: 82-2-870-2534; Fax: 82-2-870-3863; E-mail: cyho50168@naver.com.

along the axis of the stent. Double J stents manufactured by various companies have differences in the numbers and positions of side holes.

Numerical analysis has been used for the evaluation of a double J stent in the ureter, and the models for the analysis were models of a straight ureter [4-6]. However, the ureter in the human body is not straight but curved due to its location in the abdominal and pelvic cavities. Therefore, the studies performed on the models of a straight ureter might not reflect urine flow in the ureter exactly. The model of a curved ureter was made in our previous study and used for the numerical analysis of the urine flow in a stented ureter.

The role of the side holes of a double J stent is in the supply of detours in a stented ureter. The role was well seen at the side holes around an in-stent stenosis in a study using a straight ureter model [6], but it was not seen at the side holes far from the stenosis or in a case of no ureteral or in-stent stenosis. However, the side holes of a double J stent placed in the curved ureter could present different features in flow pattern, regardless of a ureteral or in-stent stenosis. Here, we made models of the curved stented ureter and evaluated the effect of the number and positions of side holes on urine flow rate and flow pattern.

2. Methods

2.1. Modeling of stented ureters (Figure 1)

The model of a curved ureter made based on the human anatomy in a previous study was used as a backbone. The diameter and length of the ureter was 4.57 or 3 mm and 226.21 mm. The renal pelvis and bladder were connected to the ureter. These shapes were a funnel and a dome with base and apex diameters and a height of 40 mm, 4.57 or 3 mm, and 15.5 mm, respectively. A CFD simulation with the upper urinary tract, including the renal pelvis, ureter and bladder, was performed.

A double J stent consists of two coils and a shaft. It has multiple side holes along the axis of the stent. Here, the side holes and end holes in the proximal and distal coils would be called ports to be

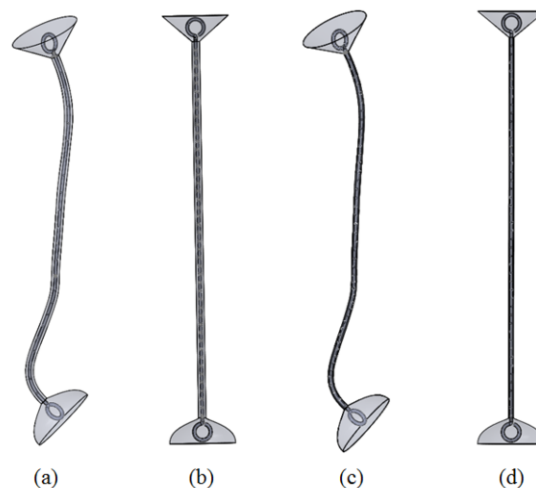


Fig. 1. Models of curved (a, c) and straight (b, d) stented ureters. They have the ureteral diameter of 4.57 mm (a, b) or 3 mm (c, d).

differentiated from the side holes in the shaft. The outer and inner diameters of the stent were 2 mm and 1 mm, respectively. The shaft was 226.21 mm, as long as the ureter. Each coil had a diameter of 10 mm and was round with five ports. The diameter of the side holes and ports was 1 mm, and 10 different types of stents with regard to the number and position of side holes were modeled (Table 1). The first is a stent with no side holes in a shaft. The others are stents with different numbers (11, 22, 45) and angular rotations (45° , 90° , 180°) of side holes. The stent goes along the axis of the ureter and is always located in the center of ureter on an axial cross section. Additionally, a straight ureter was modeled for a comparison with the curved ureter. The ureters have the same diameter and length.

2.2. Governing equations for fluid flow and numerical simulations

The governing equations, continuity equation and Navier-Stokes equation, were converted to algebraic equations by the discretization method using the finite volume method. To investigate the flow phenomenon in the ureter, Ansys CFX was used and CFX codes used a pressure-based AMG coupled solver. The continuity and momentum equations are shown in equations (1)–(2), where ρ , μ , \vec{u} , and p are density, dynamic viscosity, velocity vector, and pressure, respectively. The Semi Implicit Method for Pressure Linked Equations (SIMPLE) algorithm treats the pressure terms in the momentum equations and describes the iterative procedure by which the solution to the discretized equations is obtained [7]. Stents and ureter walls were set to be rigid with a no-slip condition imposed

Table 1
Straight and curved ureters with different types of double J stents

Case	Ureter	Number of side holes	Angular positions of side holes	Interval of side holes
1	Straight	0	-	-
2	Straight	11	0° , 180°	2 cm
3	Straight	11	0° , 90° , 180° , 270°	2 cm
4	Straight	11	0° , 45° , 90° , 135° , 180° , 225° , 270° , 315°	2 cm
5	Straight	22	0° , 180°	1 cm
6	Straight	22	0° , 90° , 180° , 270°	1 cm
7	Straight	22	0° , 45° , 90° , 135° , 180° , 225° , 270° , 315°	1 cm
8	Straight	45	0° , 180°	0.5 cm
9	Straight	45	0° , 90° , 180° , 270°	0.5 cm
10	Straight	45	0° , 45° , 90° , 135° , 180° , 225° , 270° , 315°	0.5 cm
11	Curved	0	-	-
12	Curved	11	0° , 180°	2 cm
13	Curved	11	0° , 90° , 180° , 270°	2 cm
14	Curved	11	0° , 45° , 90° , 135° , 180° , 225° , 270° , 315°	2 cm
15	Curved	22	0° , 180°	1 cm
16	Curved	22	0° , 90° , 180° , 270°	1 cm
17	Curved	22	0° , 45° , 90° , 135° , 180° , 225° , 270° , 315°	1 cm
18	Curved	45	0° , 180°	0.5 cm
19	Curved	45	0° , 90° , 180° , 270°	0.5 cm
20	Curved	45	0° , 45° , 90° , 135° , 180° , 225° , 270° , 315°	0.5 cm

on each wall. The fluid velocity at all fluid-solid boundaries is equal to that of the solid boundary [8]. When we were aiming for a steady solution, the residual of the solution with velocity and pressure converged was less than 10^{-6} .

$$\nabla \cdot \vec{u} = 0 \quad (1)$$

$$\rho \left[\frac{\partial \vec{u}}{\partial t} + (\vec{u} \cdot \nabla) \vec{u} \right] = -\nabla p + \mu \nabla^2 \vec{u} \quad (2)$$

The urine viscosity and density of 0.654 mPa·s and 1,003 kg/m³ were applied here. The urine used in the numerical simulation is similar to water in density and dynamic viscosity because most urine consists of water. The density and dynamic viscosity of urine are 1,003–1,035 kg/m³, 0.635–0.797 mPa·s at a temperature of 37°C. The viscosity is changing according to temperature, but the change is negligible in the range of body temperature 35–40.5°C, and the urine could be considered a non-compressible and Newtonian fluid. Pressure was used for the boundary condition here, where the inlet (48.9, 97.8, 195.6 Pa) and outlet (0 Pa) were specified according to reference data [6]. It was for all the 40 models to enable the comparison between the models.

To generate meshes in the ureter models, the same size of mesh was set up, and prism mesh was used for the ports of stent coils and the side holes of a stent shaft. The meshes were generated with Ansys ICEM. The greater the number of side holes, the smaller the area for meshing. In this research, the geometry of stent and hole is complex and so meshes were only made into tetrahedrons. Therefore, the number of nodes and elements for a model depended on the model types, and the number of nodes ranged from 1 million to 2.5 million, while that of elements ranged from 5.7 million to 14.5 million. These are used in the solver to construct control volumes.

3. Results and discussion

3.1. Total flow rate

The total flow rates in straight and curved stented ureters with 10 different types of double J stents are shown in Figures 2 and 3. A higher total flow rate was exhibited in straight stented ureters than in curved stented ureters, while stented ureters with multiple side holes demonstrated a higher total flow rate than those with no side holes. A higher total flow rate was exhibited in stents with more side holes, with the highest in a stent with 45 side holes and the lowest in a stent with 11 side holes. However, there was no difference in the total flow rate according to different angular rotations of side holes. The tendencies were presented regardless of ureter diameters, 4.57 or 3 mm, and were also demonstrated and exaggerated in the data achieved after doubling and quadrupling the pressure difference at the inlet and outlet boundary.

3.2. Individual flow rate

The luminal, extraluminal, and total flow rates in a curved stented ureter with a diameter of 4.57 mm (case 19, pressure difference of 48.9 Pa) is demonstrated in Figure 4 and the flow pattern around some specific ports and side holes in the ureter is shown in Figure 5. The luminal flow rate was very small compared to the extraluminal flow rate in the ureter. Urine in the renal pelvis flowed into the stent mainly through the fourth and fifth ports and the first side hole and luminal and extraluminal

flow rates were stabilized and maintained in the ureter. In the distal ureter and the bladder, urine flowed out of the stent through the last side hole and the fifth and fourth ports and the luminal flow rate became zero at the first port, which is an end hole of the coil.

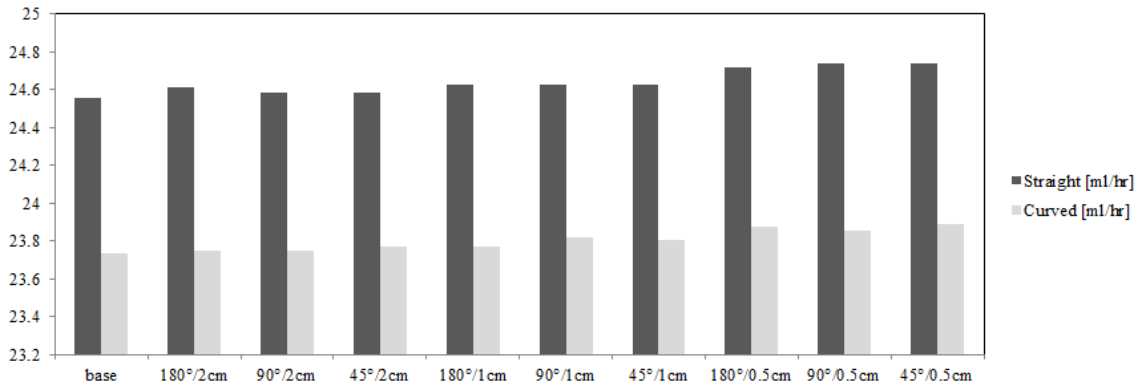


Fig. 2. Total flow rates in straight and curved stented ureters (ureteral diameter of 4.57 mm, pressure difference of 48.9 Pa).

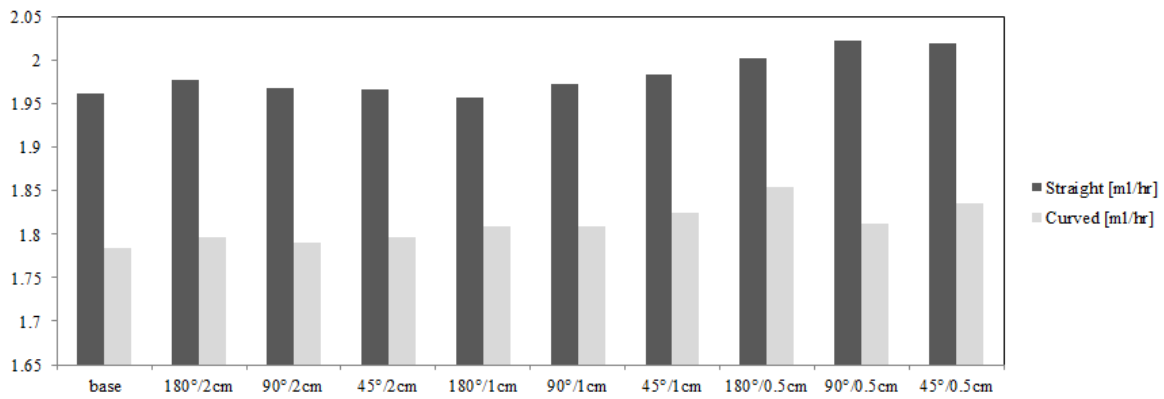


Fig. 3. Total flow rates in straight and curved stented ureters (ureteral diameter of 3 mm, pressure difference of 48.9 Pa).

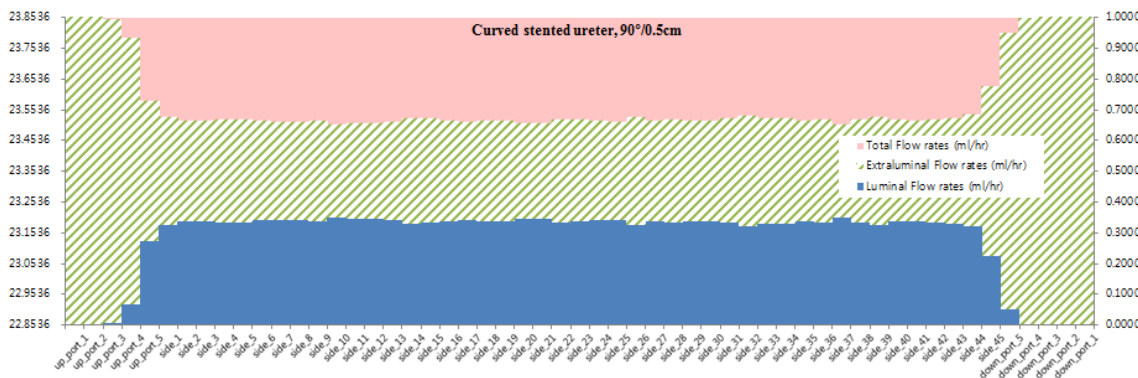


Fig. 4. Luminal, extraluminal, and total flow rates in a curved stented ureter of a 4.57 mm diameter (case 19, pressure difference of 48.9 Pa). The scale on the right Y-axis is for luminal flow rates.

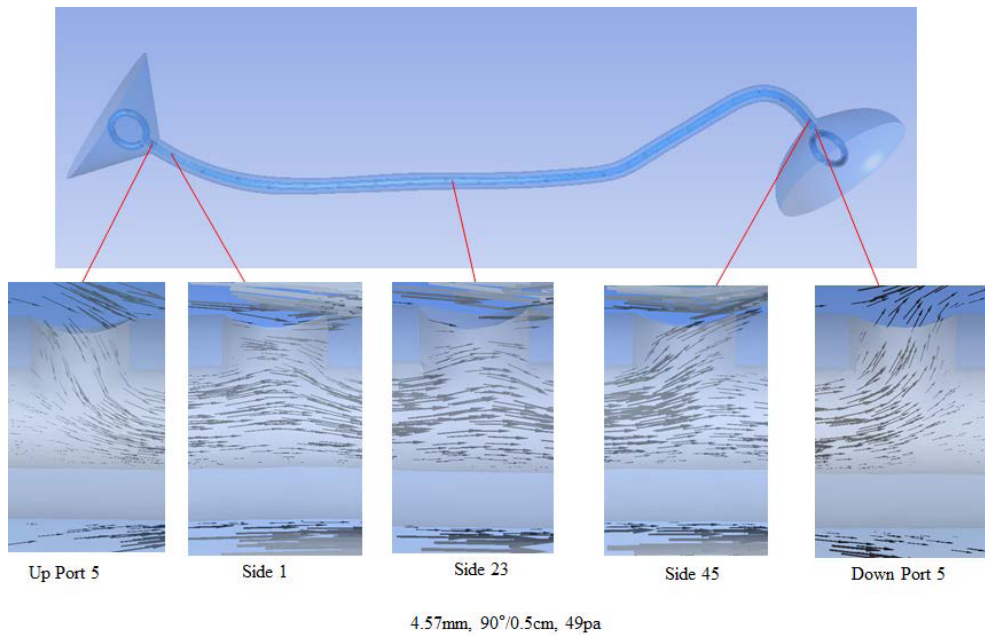


Fig. 5 Flow pattern around ports and side holes in the renal pelvis, ureter, and bladder with the ureteral diameter of 4.57 mm (case 19, pressure difference of 48.9 Pa).

In a curved stented ureter with a diameter of 3 mm (case 19, pressure difference of 48.9 Pa), the luminal flow rate was not so small compared to the extraluminal flow rate in the ureter (Figure 6). The increase, maintenance, and decrease of the luminal flow rate through the ports and side holes in the renal pelvis, ureter, and bladder was nearly same as in the ureter with a diameter of 4.57 mm (Figure 7). A small ureteral diameter encouraged urine to flow through the stent and increased the luminal flow rate relative to the extraluminal flow rate, and this could be associated with the role of a double J stent in ureteral stenosis or occlusion. However, the absolute values of luminal flow rates in the ureters with diameters of 4.57 mm and 3 mm were nearly same.

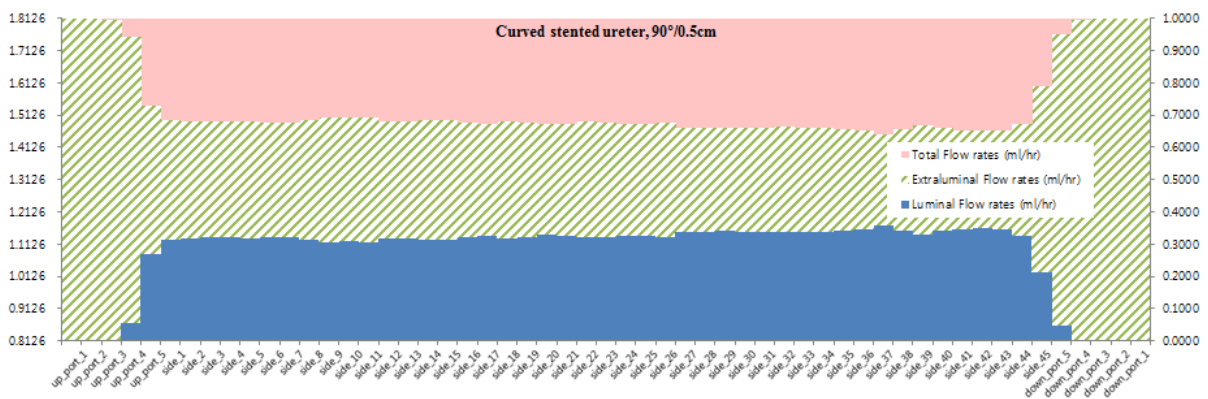


Fig. 6. Luminal, extraluminal, and total flow rates in a curved stented ureter of a 3 mm diameter (case 19, pressure difference of 48.9 Pa). The scale on the right Y-axis is for luminal flow rates.

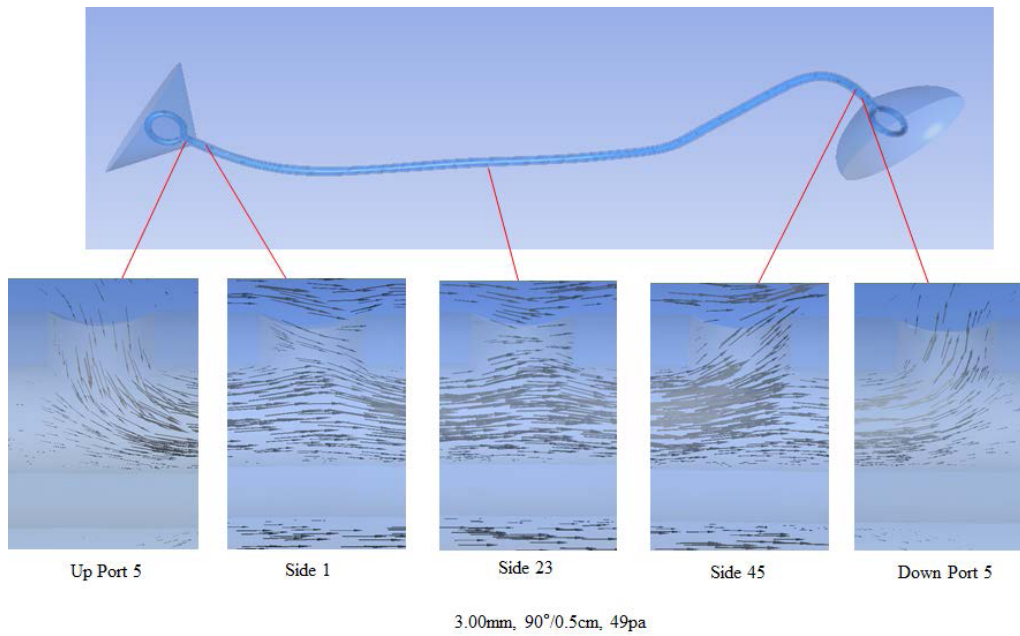


Fig. 7. Flow pattern around ports and side holes in the renal pelvis, ureter, and bladder with a ureteral diameter of 3 mm (case 19, pressure difference of 48.9 Pa).

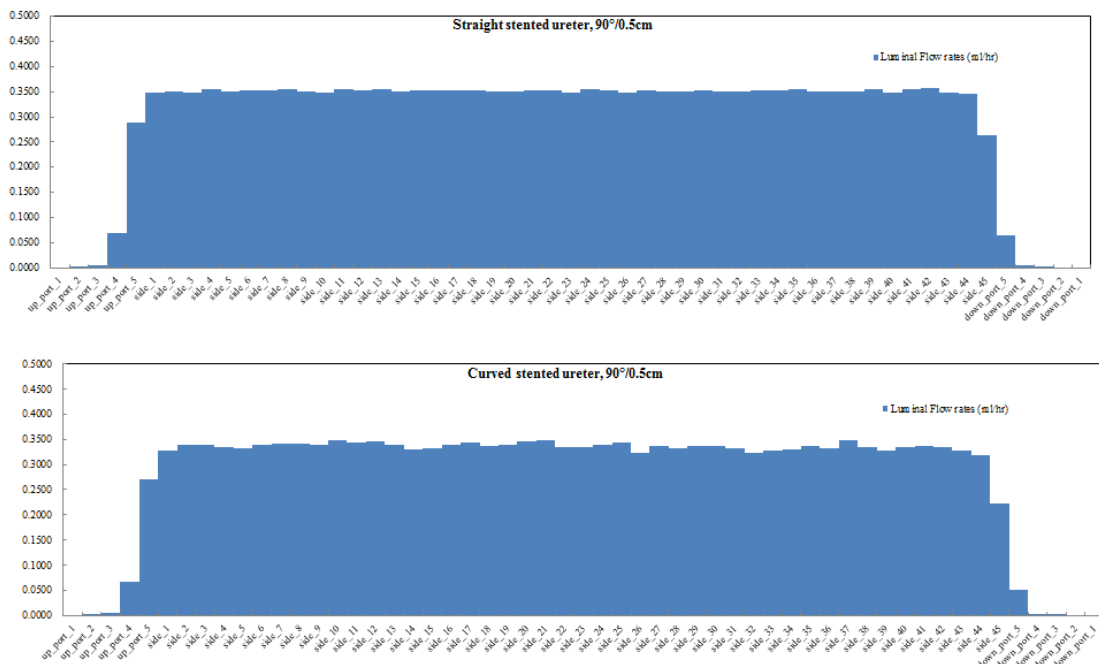


Fig. 8. Luminal flow rates in straight and curved stented ureters with a diameter of 4.57 mm (cases 9 and 19, pressure difference of 48.9 Pa).

Figure 8 demonstrates the fluctuation in the luminal flow rate in straight and curved stented ureters. The fluctuation range was greater in the curved ureter than in the straight ureter, which could result from the ureteral curvature, the factor that differentiated the straight and curved ureters. Other geometric factors including diameter and length are the same. The role of side holes in a double J stent might be expressed remarkably in the model of a curved stented ureter. It could be a good reason for the use of the curved ureter model based on human anatomy for CFD simulation; further, if the simulation is used in a clinical setting, the customized curved model based on a patient's anatomy should be used.

The fluctuation of the luminal flow rate was demonstrated even in a straight ureter. In a stented ureter, the luminal flow rate is determined by the flow through a few ports and the first side hole in the renal pelvis and proximal ureter and maintained along the ureter. Especially, in a straight stented ureter, there is no reason for a detour to occur through the side holes in the mid-ureter in a condition of no ureteral stenosis. Tong, et al. [6] reported there was no inflow or outflow to the stent lumen in the mid-ureter when there was no ureteral stenosis or stent encrustation. However, it was not revived in the current study.

In this study, the total flow rate in the ureter was achieved when there was no a double J stent inserted. The rates were 122.2 and 124.8 ml/hr in the curved and straight ureters, respectively, with a diameter of 4.57 mm and pressure difference of 48.9 Pa. The rates were 22.7 and 23.2 ml/hr in the curved and straight ureters, respectively, with a diameter of 3 mm and pressure difference of 48.9 Pa. The total flow rate in the straight ureter was greater than that in the curved ureter. Considering the rates were 23.6–24.8 ml/hr and 1.7–2 ml/hr in the stented ureters with diameters of 4.57 and 3 mm, respectively, stent placement itself must be a great obstacle, disturbing urine flow in the upper urinary system. Careful clinical judgement is necessary to determine the use of a double J stent in a patient with a ureteral stenosis or ureteral stones.

4. Conclusions

With the results, it could be stated the role of side holes in a double J stent exists even in the ureter without ureteral stenosis or occlusion and even in the model of a straight ureter. In addition, the number of side holes seemed to be important in the enhancement of total flow rate. However, the degree of the enhancement by side holes is small in a condition of no ureteral or in-stent stenosis and it might be negligible. Therefore, a further study using ureter models with stenosis is necessary to magnify the role of the side holes of a double J stent.

Acknowledgment

This research was supported by the Basic Science Research Program through the National Research Foundation of Korea (NRF) funded by the Ministry of Science, ICT & Future Planning (2014R1A1A1003987).

References

- [1] H.H. Chung, K.D. Kim, J.Y. Won, J.H. Won, S.B. Cho, T.S. Seo, S.W. Park and B.C. Kang, Multicenter experience of the newly designed covered metallic ureteral stent for malignant ureteral occlusion: comparison with double J stent insertion, *Cardiovascular Interventional Radiology* **37** (2014), 463-470.
- [2] A. Al-Aown, I. Kyriazis, P. Kallidonis, P. Kraniotis, C. Rigopoulos, D. Karnabatidis, T. Petsas and E. Liatsikos, Ureteral stents: New ideas, new designs, *Therapeutic Advances in Urology* **2** (2010), 85-92.
- [3] N. Venkatesan, S. Shroff, K. Jayachandran and M. Doble, Polymers as ureteral stents, *Journal of Endourology* **24** (2010), 191-198.
- [4] L.J. Cummings, S.L. Waters, J.A. Wattis and S.J. Graham, The effect of ureteric stents on urine flow: Reflux, *Journal of Mathematical Biology* **49** (2004), 56-82.
- [5] B. Vahidi and N. Fatourae, A numerical simulation of peristaltic motion in the ureter using fluid structure interactions, *Proceedings of the 29th Annual International Conference of the IEEE EMBS, Cite Internationale, Lyon, France, 2007*, pp. 1168-1171.
- [6] J.C. Tong, E.M. Sparrow and J.P. Abraham, Numerical simulation of the urine flow in a stented ureter, *Journal of Biomechanical Engineering* **129** (2007), 187-192.
- [7] S. Patankar, *Numerical Heat Transfer and Fluid Flow*, CRC Press, Boca Raton, Florida, USA, 1980, pp. 126-131.
- [8] M.A. Day, The no-slip condition of fluid dynamics, *Erkenntnis* **33** (1990), 285-296.